THE ZEEMAN EFFECT IN THE RED CaH BANDS

By William W. Watson and William Bender
Sloane Physics Laboratory, Yale University

(Received May 1, 1930)

Abstract

The Zeeman effect in the red $^2\Pi \rightarrow {}^2\Sigma$ and $^2\Sigma \rightarrow {}^2\Sigma$ CaH bands, together with new satellite branches in the $^2\Pi \rightarrow {}^2\Sigma$ system, are reported. Field strengths up to 30,000 gauss were employed, the dispersion of the large concave grating in a parallel light mounting being about 2.1A per mm.

Satellite series in the $^2\Pi \rightarrow {}^2\Sigma$ bands.—The ${}^0P_{12}$ satellite branches are measured for both the A and A' bands. These frequencies together with certain combination relations fix the hitherto uncertain J numbering in the Q branches, and hence the size of the Λ-type doubling. This doubling is very large (70 cm^{-1} at $K=34\frac{1}{2}$) and of opposite sign to that usually found in other bands.

Zeeman effect in the $^2\Pi \rightarrow {}^2\Sigma$ bands.—General agreement with the pattern blocks predicted by Hill's theoretical formulas for the lower K' states is found. Intensity variations with increasing field strength are described. For $K'>19$, where the no-field spin doublet components come together and cross over, uncoupling effects occur. Only the transitions from anti-parallel S and K in the $^2\Pi$ state to parallel S and H in the $^2\Sigma$ state, and from parallel S and K to antiparallel S and H persist. The displacements of these components are proportional to H^2. At 30,000 gauss the high K components in the P_1 branch broaden out and go rapidly to zero intensity, but the P_2 field components remain narrow and strong. With complete uncoupling by this "strong field," these components are probably the transitions from parallel S and H in the $^2\Pi$ state to parallel S and H in the $^2\Sigma$ state. For the highest K levels, these high-field P_2 components are displaced farther from the no-field position and become more diffuse, suggestive of an approach to Hund's case d.

Zeeman effect in the $^2\Sigma \rightarrow {}^2\Sigma$ bands.—Contrary to the usual findings for bands of this type, broad and prominent Zeeman patterns here occur for $K'>8$ which are quite similar to those found in a $^2\Pi$ state. The explanation is probably that an appreciable magnetic moment is created in the upper $4s\sigma^2 3d\sigma\ ^2\Sigma$ state by the increasing component of L along the rotational axis.

Introduction

A THEORETICAL treatment of the Zeeman effect in doublet band spectra has recently been published by E. L. Hill,[1] and the formula for the magnetic field patterns have been nicely verified by Almy and Crawford[2] for the case of the MgH $^2\Pi \rightarrow {}^2\Sigma$ band system. This theory considers molecules which can be classed under Hund's cases (a) and (b) or for cases intermediate between (a) and (b), neglects "rho-type" doubling, and considers the only uncoupling effect to be that on the electron spin. There are examples of diatomic molecules, however, where the rho-type doubling becomes very large, and where the coupling of the electronic orbital angular momentum to the rotational axis would be accompanied by a magnetic

[1] E. L. Hill, Phys. Rev. **34**, 1507 (1929).
[2] G. M. Almy and F. H. Crawford, Phys. Rev. **34**, 1517 (1929).

moment in that direction. In the $\lambda 6389\,^2\Sigma \rightarrow {}^2\Sigma$ and $\lambda 7000\,^2\Pi \rightarrow {}^2\Sigma$ CaH bands, for which these effects become very large, the Zeeman effect predicted by Hill's theory is to be expected, then, for the lower rotational states, but for the highest rotational states new magnetic field patterns should be found. Measurements of this perturbing effect of an external field should increase our knowledge of the dynamics of molecules exhibiting such a very large ρ-type and Λ-type doubling.

The analysis of Hulthén,[3] together with Mulliken's[4] discussion of these data, demonstrate the marked distortion increasing with the rotation in these CaH bands. In the upper electronic state of the $^2\Sigma \rightarrow {}^2\Sigma$ band the orientation energy of the spin S with respect to the nuclear rotation axis, as measured by the separation of the F_1 and F_2 terms, is exceptionally large, the rotational doublets being separated even at the origin of the band by 1.3 cm^{-1}. Also the usual relation for $^2\Sigma$ states, $F_1 > F_2$, is reversed in this case. In the $^2\Pi$ state of the $\lambda 7000$ band the Λ-type doubling is very large (see below), thereby indicating a large L_{perp} (component of orbital angular momentum L perpendicular to the electric axis of the molecule), and the usual $^2\Pi$ state relation, $F_2(J) > F_1(J+1)$, which does hold for low J values is reversed for $J > 19\frac{1}{2}$. The ρ-type doubling in the common lower $^2\Sigma$ state is small, as in most $^2\Sigma$ states.

Experimental Procedure

Our source was an intermittent d.c. arc in a modified Back chamber mounted on the pole faces of a large water-cooled Weiss electromagnet. The moving electrode was a small block of metallic calcium mounted on a tungsten wire, while the fixed electrode was a thin copper strip insulated from the pole face by a piece of mica. The arc was struck in a hydrogen atmosphere at from 5 to 10 cm pressure, and since the arc chamber was not absolutely vacuum tight, a stream of hydrogen gas from a tank was pumped slowly through the apparatus during the exposures. It was necessary to renew the calcium electrode at frequent intervals during each run. The bands were photographed in the second order of a large concave grating mounted in parallel light, the dispersion being approximately 2.1A per mm.

The $\lambda 6389$ band was photographed with Eastman panchromatic plates hypersensitized by an ammonia bath. Plates were taken with field strengths of 14,000, 24,600 and 29,950 gauss with no polarizing prism in the path, and at 29,950 gauss in the perpendicular and parallel polarizations separately, with the exposure times up to 12 hours when the Nicol prism was used. The $\lambda 7000$ band was recorded on Eastman 40 and panchromatic plates dyed with dicyanin. Field strengths of 10,500 and 30,000 gauss were used, the times of actual exposure on the slit running to 18 hours. On every plate in addition to the field exposure a no-field comparison and an iron arc spectrum were photographed. The strength of the magnetic field was determined by measurements of the patterns of the Zn triplet $\lambda\lambda 4680$, 4722, and 4811.

[3] E. Hulthén, Phys. Rev. **29,** 97 (1927).

[4] R. S. Mulliken, Phys. Rev. **30,** 138 (1927), and **32,** 388 (1928).

New Series and Magnitude of Λ-type Doubling in $^2\Pi \rightarrow {}^2\Sigma$ Band

The J values assigned by Hulthén[3] to the lines in the P and R branches of the λ7000 band are correct when reduced by $\frac{1}{2}$ unit in order to agree with the quantum mechanics numbering. But since it is apparent from Hulthén's data that the ordinary PQR combination relation does not even hold approximately, and since no (1, 0) or (0, 1) band seems to be available for combination checking purposes, the J numbering in the Q branches has been heretofore undetermined. Now our spectrograms indicate that all the satellite series to be expected in a $^2\Pi_{ab}$ state[5] are present and with fair intensity in this band. In particular the $^0P_{12}$ satellite branch[6] proceeds to the red from the P branch head in a region clear of other lines. The frequencies of the lines in this branch can be calculated from the relation[7]

$$\begin{aligned} {}^0P_{12}(J) &= Q_1(J-1) + [F_1''(J-1) - F_2''(J-2)] - [F_2''(J) - F_2''(J-2)] \\ &= Q_1(J-1) + 0.045(J - 1\tfrac{1}{2}) - \Delta_2 F_2''(J-1). \end{aligned} \quad (1)$$

The second term on the right side of this equation involves the empirical rule for the separation of the spin components in the lower state of these bands,[5] while the $\Delta_2 F_2''$ values can be taken directly from Hulthén's tables. The proper Q_1 frequencies to so combine with these F'' differences as to give the observed satellite branch lines can be thus uniquely determined, and the important point is that this fixes the J numbering of the Q_1 branch and hence the exact course of the Λ-type doubling in the F_1' levels. Table I

Table I. $^0P_{12}$ *Series in* (0,0) *and* (1,1) *CaH* $^2\Pi \rightarrow {}^2\Sigma$ *bands.*

	(0,0) or A band		(1,1) or A' band	
J	ν calc.	ν obs.	ν calc.	ν obs.
$11\frac{1}{2}$	14231.68	14231.58		
$12\frac{1}{2}$	18.66	18.62		
$13\frac{1}{2}$	06.17	05.88		
$14\frac{1}{2}$	193.77	193.48		
$15\frac{1}{2}$	81.55	81.36		
$16\frac{1}{2}$	69.69	69.61	14209.91	14209.78
$17\frac{1}{2}$	58.23	58.08	198.66	198.55
$18\frac{1}{2}$	47.12	46.94	87.81	87.54
$19\frac{1}{2}$	36.21	36.07	77.28	76.92
$20\frac{1}{2}$	25.86	25.61	66.92	66.75
$21\frac{1}{2}$	15.78	15.49	56.97	56.60
$22\frac{1}{2}$	06.02	05.72	47.36	—
$23\frac{1}{2}$	096.53	96.36	38.17	37.84
$24\frac{1}{2}$	87.64	087.35		
$25\frac{1}{2}$	78.97	78.68		
$26\frac{1}{2}$	70.73	70.51		
$27\frac{1}{2}$	62.56	62.70		

[5] Cf. R. S. Mulliken, Phys. Rev. **32,** 388 (1928) for a detailed account of the various possible branches in $^2\Pi \rightarrow {}^2\Sigma$ transitions.

[6] We are using, throughout, the notation recommended by R. S. Mulliken in his forthcoming article in this journal on standardized notation for description of molecular spectra. This branch would be designated formerly as $^{PP}P_{12}$.

[7] Compare level diagram in ref. 5. Note particularly that the $^0P_{12}$ and Q_1 transitions are from the same A sublevels in the upper state.

gives the wave-numbers of the observed ${}^0P_{12}$ lines for both the (0, 0) and (1, 1) bands together with their calculated values from Eq. (1). The agreement of the observed and calculated frequencies can only be produced by increasing Hulthén's J numbering in the Q_1 branch of the (0, 0) band (his A band) by $1\frac{1}{2}$ units, and in the Q_1 branch of the (1, 1) band (his A' band) by $\frac{1}{2}$ unit. Two new Q_1 lines should be added to Hulthén's tabulation for the A band; $Q_1(\frac{1}{2})$ 14393.31 and $Q_1(1\frac{1}{2})$ 14396.71. These are clearly present and of good intensity on our plates. Because of the confusion of stronger lines in the short wave-length side of these bands, the accurate measurement of the corresponding ${}^SR_{21}$ is rendered difficult. Fragments of this branch have been located, however, and seem to indicate similarly that Hulthén's J numbering in the Q_2 branch should also be raised $1\frac{1}{2}$ units. In computing the magnitude of the Λ-type doubling in the F_1' terms we use the relation

$$\begin{aligned}&[R_1(J) - Q_1(J)] - [Q_1(J+1) - P_1(J+1)]\\ &= F_{1B}'(J+1) - F_{1A}'(J) - F_{1A}'(J+1) + F_{1B}'(J)\\ &\backsimeq F_{1B}'(J+\tfrac{1}{2}) - F_{1A}'(J+\tfrac{1}{2}).\end{aligned} \qquad (2)$$

Table II gives in condensed form the course of this doubling, showing that for the lowest J levels the doubling increases in the usual fashion;[8] but that at $J=6\frac{1}{2}$ the separation of these sublevels begins to decrease, becomes

TABLE II. *Λ-type doubling in F_1' levels of* (0,0) ${}^2\Pi\rightarrow{}^2\Sigma$ *band calculated from Eq.* (2).

J	$F_{1B}'(J+\frac{1}{2})-F_{1A}'(J+\frac{1}{2})$	J	$F_{1B}'(J+\frac{1}{2})-F_{1A}'(J+\frac{1}{2})$
$1\frac{1}{2}$	+2.04	$11\frac{1}{2}$	− 0.54
$2\frac{1}{2}$	2.66	$12\frac{1}{2}$	− 1.76
$3\frac{1}{2}$	3.06	$14\frac{1}{2}$	− 4.61
$4\frac{1}{2}$	3.26	$19\frac{1}{2}$	−14.00
$5\frac{1}{2}$	3.27	$24\frac{1}{2}$	−25.89
$6\frac{1}{2}$	3.06	$29\frac{1}{2}$	−53.38
$9\frac{1}{2}$	1.45	$34\frac{1}{2}$	−69.71
$10\frac{1}{2}$	+0.53		

zero at $J=11\frac{1}{2}$, and increases to very large negative values for the highest rotational levels. The F_2' levels proceed apparently in much the same way, although usually[8] F_2 levels show an almost negligible Λ-type doubling.

This large rotational doubling in the Π state is evidence for a very considerable growth in L_{perp}. There is reason therefore for supposing that the effect of an external magnetic field on these high rotational levels would be a variation of that for cases a to b.

THE ZEEMAN EFFECT IN THE ${}^2\Pi\rightarrow{}^2\Sigma$ BAND

We will consider the effect of the magnetic field first for the lines of low and intermediate K values, and then for the high rotation lines. For the lines in the first group the CaH molecule is intermediate between case a and case b, and Hill's theory should give a good description of the observed patterns. Since the ρ-type doubling is small in the lower ${}^2\Sigma$ state, the only effect of the field in this state should be to uncouple the spin S from its weak coupling with K, so that these levels all become sharp doublets of separation

[8] J. H. Van Vleck, Phys. Rev. **33**, 467 (1929). R. S. Mulliken, Phys. Rev. **33**, 507 (1929).

$2\Delta\nu_{norm}$. In general one must make a detailed computation with Hill's equation (22), the constants for our $^2\Pi$ state being $B=4.3\ cm^{-1}$, $\lambda=+19\ cm^{-1}$, $\Lambda=1$. Since for no line have we observed the resolved magnetic fine structure due to all the possible values of M, the magnetic quantum number, it is only necessary to calculate the position and overall widths of the blocks of unresolved components in the patterns by using $M=+J$, 0, and $-J$. These patterns we have calculated for $K'=3$, 10, and 18. For $K'=18$, and even for $K'=10$, Hill's energy equation considerably overestimates the width of the spin doublet interval, since it does not consider ρ-type doubling, and therefore complete quantitative agreement with the observations is not to be expected. The details of the comparison, together with some observations on lines with approximately these K' values are presented in Table III. Figs. 1 and 2 show graphically this comparison for $K'=3$ and 10.

TABLE III. *Comparison of observed and calculated patterns for low and intermediate values of K in $^2\Pi\rightarrow{}^2\Sigma$ band.*

(In this and the other tables + indicates field radiation to the higher frequency side, − to the lower frequency side, of the no-field position.)

Lines	Patterns
$P_1(2\frac{1}{2})$, $(4\frac{1}{2})$ $(5\frac{1}{2})$, $(6\frac{1}{2})$	$K'=1$ to 5
	$H=10{,}500$ gauss, $\Delta\nu_n=0.49\ cm^{-1}$. Theory predicts at $K'=3$ a symmetrical doublet, with $0.98\ cm^{-1}$ between centers of the two component blocks, separation between "inside" edges 0.61, width of each component 0.38;
$Q_1(2\frac{1}{2})$, $(4\frac{1}{2})$, $(5\frac{1}{2})$ $R_1(2\frac{1}{2})$, $(3\frac{1}{2})$	Obs. doublet width
	K' | P | Q | R — Measurements from center to center showing that since obs. width <theoretical, inside edges are stronger. Components same intensity for $K'1$ and 2, but red component then becomes stronger, and at $K'=5$ is much stronger than violet component.
	1 | 0.78 | | —
	2 | | 0.84 | —
	3 | | | 0.71
	4 | 0.83 | 0.70 | 0.74
	5 | 0.80 | | —
	$H=30{,}000$ gauss, $\Delta\nu_n=1.41$. Calculated pattern wide diffuse doublet, approx. symmetrical about no-field position; roughly in agreement with obs. $P_1(4\frac{1}{2})$ pattern. − components inside edge at −0.89; obs. −0.94. Violet block's outermost edge at +1.93; obs. +2.06. Other two edges obscured. Q_1 lines also become diffuse doublets but the intensity distribution is very different: the two blocks are of equal intensity, whereas at the lower field strength the "wings" are more intense; maximum intensity in each block is near the inner edge, nearest the no-field position. Red component's maximum at −0.72, violet's at +0.79, whereas predicted inside edges are −0.89 and $+0.85\ cm^{-1}$.
	$K'=9$ to 14
$P_1(11\frac{1}{2})$, $(12\frac{1}{2})$ $(13\frac{1}{2})$ $Q_1(10\frac{1}{2})$, $(13\frac{1}{2})$ $P_2(9\frac{1}{2})$, $(10\frac{1}{2})$, $(11\frac{1}{2})$ $Q_2(13\frac{1}{2})$	$H=10{,}500$. Calculated patterns are doublets. F_1 states: calculated inside edge of red component at −0.08 for $K'=10$; obs. −0.09 −0.08, −0.14 for $P_1(11\frac{1}{2})$, $P_1(12\frac{1}{2})$, and $Q_1(10\frac{1}{2})$ respectively. Width of red components: calc., 0.78; obs., 0.39, 0.35, and 0.30 respectively—i.e., obs. blocks much narrower than calculated width. P_1 and R_1 violet components of negligible intensity, but in $Q_1(10\frac{1}{2})$ the violet component is weaker than the red component but is present starting at the red component and extending to +0.51, against the theoretical max. displacement +0.90. F_2 states: Predicted doublets are approximately symmetrical with respect to no-field line, have components narrower, $0.48\ cm^{-1}$, and separated by $0.98\ cm^{-1}$ between centers for $K'=10$. Observed patterns in good agreement with theory. Violet or "wing" components much stronger than red components and narrower than predicted.

TABLE III (*continued*).

Observed F_2 Patterns

	K'	Doub. width	Component widths	
P_2	9	0.85	−0.37	+0.28
Q_2	14	0.79	−0.46	+0.31

H= 30,000. F_1 *states*: Lines should become broad symmetrical doublets in field according to theory. P_1 and R_1 patterns not present; probably too weak and diffuse. Q_1 lines become strong broad doublets, narrowing with increasing K, and whose inside edges nearest the no-field line are much the stronger parts of the patterns. For K'= 10 these maxima are at −0.50 and +0.55 as against computed inside edges for the blocks at −0.28 and +0.30 The red "wing" components are just as intense as the violet components.

F_2 *states*: Calculated field doublets are symmetrical, have inside edges farther from no-field position, and have narrower component blocks. All in agreement with observations, but obs. components much narrower than predicted, hence quite intense; also two components are equally strong.

P_2 component separations from no-field line.

K'	Calc.	Obs.−	Obs.+
9		1.14 to 1.62	1.08 to 1.37
10	0.74 to 2.08	1.15 to 1.45	1.05 to 1.34
11		1.17 to 1.57	0.98 to 1.31

K'= 18

$P_1(19\frac{1}{2})$ $Q_1(18\frac{1}{2})$ $P_2(18\frac{1}{2})$ $R_2(16\frac{1}{2})$

H= 10,500. According to theory all lines become doublets in the field; the F_1 patterns with very narrow components separated by 0.96. Actually only the red "wing" components can be seen; in $P_1(19\frac{1}{2})$ from −0.08 to −0.43; in $Q_1(18\frac{1}{2})$ from +0.01 to −0.29, although theory has this component at −0.48.

F_2 patterns are calculated to be more diffuse doublets with but 0.21 cm^{-1} between inside edges and center of components at −0.48 and +0.50. For $P_2(18\frac{1}{2})$ only violet component observed from +0.07 to +0.38. $R_2(16\frac{1}{2})$ becomes a doublet with strong violet component from +0.16 to +0.46 and very weak red component at −0.27. Theory predicts no-field spin doublet separation 15.8 cm^{-1}, whereas experimentally it is but 2.5 cm^{-1}.

H= 30,000. Theory predicts widely separated doublets (2.82 cm^{-1}) with components narrow for F_1 patterns. These are not observed. No P_1R_1 field radiation is apparent and the Q_1 pattern is broad and diffused into adjacent patterns. F_2 patterns predicted to be broad diffuse doublets with inside edges at −0.32 and +0.35 and centers at −1.30 and +1.52 for the red and violet components respectively.

Observed F_2 patterns for K'= 18

$P_2(18\frac{1}{2})$	−0.86 to −1.30	+0.94 to+1.67
$R_2(16\frac{1}{2})$	−0.86 to −1.30	+1.22 to +1.61

Both components intense and considerably narrower than the computed widths.

Some of the more striking features of the observed patterns should be emphasized. In agreement with the theory, all of these lines apparently become doublets in the field, each component of the doublet of course being in reality a block of $2J+1$ unresolved lines, but the observed doublet width is always less than that predicted. This smaller width may be caused by the relative faintness of the outer portions of the patterns. At 10,500 gauss, for all except the very lowest K' values, the intensity is almost entirely in the red components for the P_1, Q_1, R_1 patterns and in the violet components for

the P_2, Q_2, R_2 patterns. These are the transitions from parallel S and K in the $^2\Pi$ state to the $M_s = +\frac{1}{2}$ level in the $^2\Sigma$ state and anti-parallel S and K to $M_s = -\frac{1}{2}$ respectively, and correspond to the "wings" of Almy and Crawford's

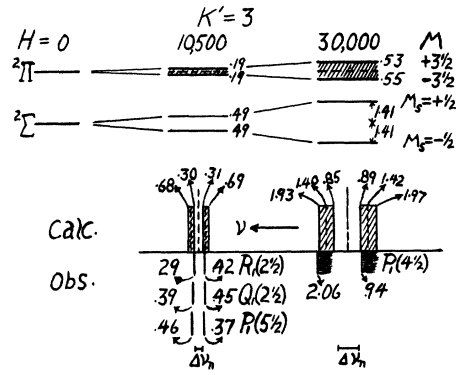

Fig. 1. Calculated splitting of the energy levels and the resulting Zeeman patterns for lines with $K'=3$ from Hill's theoretical equation (ref. 1). Of the observed lines, $P_1(4\frac{1}{2})$ and $R_1(2\frac{1}{2})$ have $K'=3$, while for $Q_1(2\frac{1}{2})$, $K'=2$ and $P_1(5\frac{1}{2})$ has $K'=4$. The corresponding P_2, Q_2, R_2 lines are too weak to observe. Since at 10,500 gauss the field components are narrow, only a measurement of the center of the component in each case was made. At 30,000 gauss due to overlapping patterns only the measurements given on the $P_1(4\frac{1}{2})$ line pattern could be made, but the observations indicate widths for the blocks approximately in agreement with the predictions.

MgH patterns.[2] The components arising from the other two possible transitions[9] we shall refer to as the "inside" components. At 30,000 gauss, however, both components are equally strong for all the patterns measured (P_2, R_2,

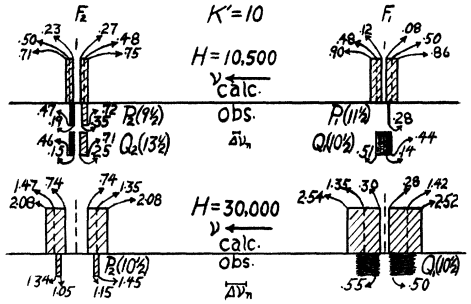

Fig. 2. Comparison of calculated and observed patterns for lines with $K'=10$. The $P_1(11\frac{1}{2})$ $Q_1(10\frac{1}{2})$ and $P_2(10\frac{1}{2})$ lines all have $K'=10$. For $P_2(9\frac{1}{2})$, $K'=9$, while for $Q_2(13\frac{1}{2})$ $K'=14$. At 10,500 gauss the "outside" components are much stronger (indicated by solid black) than the inside (shaded) components. At 30,000 gauss the P_2 components are narrower than predicted, the Q_1 components are strongest at their edges nearest the no-field line position, and both components are in all cases of equal intensity.

Q_1), thus indicating that, because the no-field spin doublet separation is still considerably greater than $\Delta\nu_n$, the coupling of S in the $^2\Pi$ state has not been

[9] Cf. the excellent diagrams illustrating the relation between the possible transitions and the components in ref. 2.

broken down by the field. The intense concentration of the patterns of the Q_1 lines as contrasted with the apparent absence of field radiation for the P_1 and R_1 lines, however, is difficult to explain. The enlargement of a portion of this band in Fig. 3 illustrates some of these pattern changes.

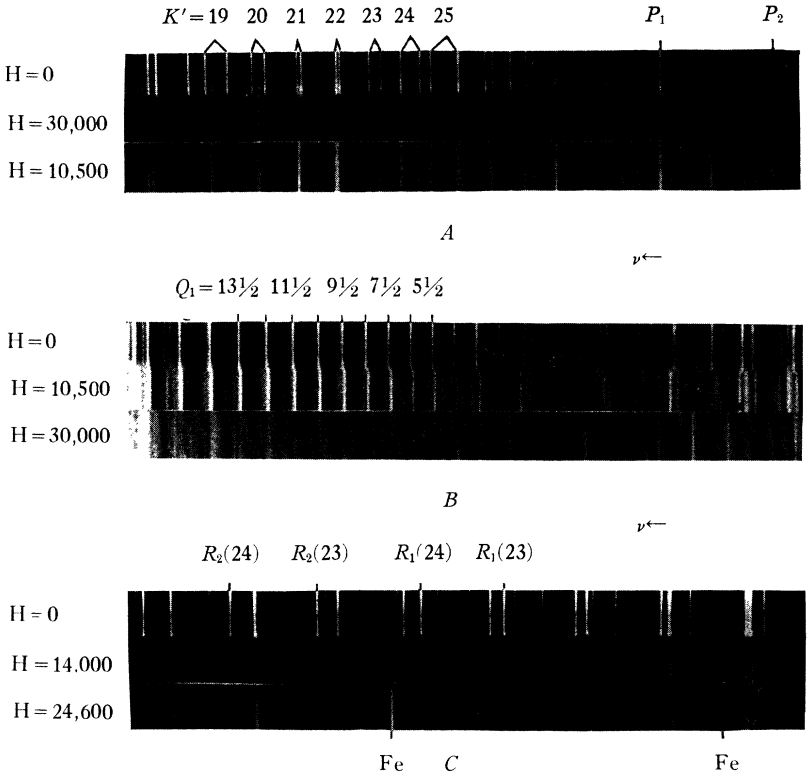

Fig. 3. Enlargements 9 times. A shows the "cross-over" region in the P branches of the $^2\Pi \rightarrow {}^2\Sigma$ band. It is evident that for $K' > 24$ both the P_1 and P_2 lines for $H = 10{,}500$ gauss have "inside" component blocks equally strong, but that for $H = 30{,}000$ gauss the P_1 field radiation has broadened out and become of negligible intensity, although the P_2 components are strong. In the reproduction P_1 and P_2 denote the heads of the two branches in the no-field strip. In B note the greater intensity of the field components on the long wave length side for $H = 10{,}500$ gauss as compared to the equal intensity of the two field components for $H = 30{,}000$ gauss. In the latter case the greater intensity of the field blocks at their inside edges is evident. C gives some of the patterns for high K values in the $^2\Sigma \rightarrow {}^2\Sigma$ band. The R_2 line patterns and the weak components of the R_1 lines on the high frequency side are of insufficient intensity to be brought out well in the reproduction. The breadth of the no-field lines in C is due to over exposure.

For $K' \geqq 19$ where the no-field spin doublet components come close together and then cross over, making $F_1'(J+1) > F_2'(J)$, prominent and interesting "second-order" or Paschen-Back effects appear. These effects are summarized in Table IV and are illustrated in Fig. 3A for the P_1, P_2 lines only. That a "strong field" uncoupling of S is here taking place is evidenced by first, the fact that the wing components decrease to zero intensity

TABLE IV. *Magnetic field patterns at and beyond the cross-over in the P branch spin doublets in the* $^2\Pi \rightarrow {}^2\Sigma$ *band.*

K'	
	10,500 gauss. $\Delta\nu_n = 0.49$ cm^{-1}
19	Practically all the intensity in the "wings". $P_1(20\frac{1}{2})$ wing at -0.28, $P_2(19\frac{1}{2})$ wing at $+0.33$. Very little shading between the lines.
20	Now wings are weaker and the other two "inside" components have appeared. Reckoning from the P_2 line: P_1 wing at -2.07, P_1 no-field, -1.64; inside components fused from -1.36 to -0.44, P_2 wing $+0.51$.
21	Wings have disappeared. P_1 no-field at -0.57, strong field component -0.52 to -0.29, weaker fused field radiation from strong component to $+0.13$.
22	No-field lines have now crossed over. Field pattern one strong broad block approximately width of original spin doublet separation, 0.51. No wings.
23	Fused inside components now separated because spin doublet separation is greater. P_2 no-field at 0.0, P_2 component at $+0.07$, P_1 component $+1.45$, P_1 no-field $+1.54$. These P_1 and P_2 field components are equally strong. No wings. Succeeding P_1 and P_2 lines to the ends of the branches similarly affected.
	30,000 gauss. $\Delta\nu_n = 1.41$ cm^{-1}
	Reckoning all separations from the P_2 no-field line position in each pattern:
19	Weak shading in field starts at P_1 no-field, -2.83, and goes to strong band component starting at -0.91 and ending -0.41, P_2 wing from $+1.74$ to $+2.20$.
20	Weak shading from -1.82 to strong component starting at -1.00 and ending -0.65. P_1 no-field position is -1.64. No evidence now of P_2 wing.
21	Rather strong shading begins sharply at -1.08 and extends to the strong, narrower field component at -0.24. P_1 no-field position is -0.57. No wings.
22	Lines have crossed. Strongest field line and $P_2(22\frac{1}{2})$ position at 0.00, with field radiation extending rather intense to a strong edge at $+0.85$. P_1 position is $+0.51$. No wings.
23	Weaker fused field radiation starts at -0.35 and extends to $+1.94$. Edges of this block are well defined. Strong field component at $+0.45$ superposed. P_1 position is $+1.54$.
24	Strong field component at $+0.54$ with weaker field radiation solid from here to $+2.88$. P_1 position is $+2.50$.
25	Strong field component at $+0.74$. Broad weak field radiation for the P_1 from $+1.75$ to $+4.47$. P_1 position is $+3.53$.
	From here on to the P_1 head, the P_1 field radiation is very diffuse and weak causing the whole background to be slightly blackened. The strong P_2 field component blocks continue out to the P_2 head, the displacements from the no-field positions for the next four lines being $+0.65$, $+0.69$, $+0.75$ and $+0.73$, or about $\frac{1}{2}\Delta\nu_n$. For the last lines near the head, the displacements are a little greater, averaging $+0.80$ cm^{-1} for $K'=36$, 37, 38, and the components are becoming definitely broader and more diffuse.

and the inside components come in strong as the spin doublet separation goes to zero. This is to be interpreted as due to the uncoupling of S from its interaction with the internal field directed along the rotational axis in the molecule, the F_2 state in which S and K are anti-parallel being replaced by the parallel orientation of S and the field H, while the F_1 state or parallel S and K is replaced by the state in which S lies anti-parallel to H.[10] S and K are then separately quantized with respect to the field, giving the quantum numbers M_S and M_K. Since only the inside components representing transitions for which $M_S=0$ occur for all levels of higher K, we infer that this uncoupling is complete. Second, the displacement of the strong P_2 field components seems to be almost exactly proportional to H^2 rather than to H as in the usual first-order Zeeman effects.

The difference between the patterns of the P_1 and P_2 lines at 30,000 gauss in this uncoupling process is striking. The one inside field component

[10] Reference 1, p. 1513.

of the P_2 lines is rather narrow and intense, whereas the field radiation associated with the P_1 lines in the interval from $K'=20$ to 25 becomes increasingly broader and weaker, and for $K'>25$ is too weak to detect. Apparently the transition from parallel S and H in the $^2\Pi$ state is very much more probable when the field is "strong" than that from the anti-parallel S and H, indicating an instability of this anti-parallel orientation.

Also to be especially noticed are the increasing separation and increasing diffuseness of these high field P_2 components for the highest K levels. This would seem to be related to the exceptionally large Λ-type doubling and consequent relatively large L_{perp}. The electric axis of the molecule at these highest rotational levels is probably becoming less effective in orienting the L, with the result that Λ is no longer a good quantum number. There is a close approach to the case d type of coupling, and the resulting changes in the magnetic moment are reflected in the broadening of these last field patterns.

The Zeeman Effect in the $^2\Sigma \rightarrow {}^2\Sigma$ Band

Neglecting ρ-type doubling, $^2\Sigma \rightarrow {}^2\Sigma$ bands should exhibit no first order Zeeman effect, for the field merely completely uncouples the spin S in both states, and with $\Delta M_S=0$ accurately holding, no displacement of the spectrum lines is to be expected. The very pronounced ρ-type doubling in the λ6389 CaH band, however, indicates a considerable energy of orientation of S with respect to an internal field directed along the rotational axis in the

TABLE V. *Summary of magnetic field measurements in the* λ6389 $^2\Sigma \rightarrow {}^2\Sigma$ *CaH band.*
($H_1=14{,}090$ gauss, $\Delta\nu_n=0.66$. $H_2=24{,}600$ gauss, $\Delta\nu_n=1.16$. $H_3=29{,}950$ gauss, $\Delta\nu_n=1.41$)

K'	Measurements and Remarks
1 to 7	P_1 and R_1 lines (parallel S) unaffected by field $R_2(1\frac{1}{2})$ becomes a doublet in field, components at -0.35 and $+0.55$ for H_2 and -0.36 and $+0.88$ for H_3

Other R_2 lines are affected by field but patterns are confused with other radiation
P_2 lines are doubled in field:

K'	H_1	H_2	H_3
1	-0.42, -0.29, $+0.62$	-0.67 to -0.27, no + comp.	-0.67 to -0.21, no + comp.
2	-0.87 to -0.26, $+0.29$ to $+0.54$	-0.28, no + comp.	—
3	-1.02 to -0.18, $+0.22$ to ?	diffuse + comp.	—
4	-0.74 to -0.12, $+0.35$ to $+0.87$	diffuse + comp. ?	from -0.24 shaded to red, strong and from $+0.53$ shaded to violet, weak

For $K''>8$ all of the R_1 and R_2 lines have the patterns as given below for a few samples:

	R_1			R_2		
	H_1	H_2	H_3	H_1	H_2	H_3
12	-0.60 to -0.25 and shades to $+0.93$	-1.34 to -0.20 and $+0.28$ to $+0.91$	-1.74 to -0.25 and $+0.42$ to ?	0.00 to $+0.76$		
		+ and − components same strength		These single blocks shading to the violet from the no-field position constitute the full R_2 pattern		
15	−comp. at -0.44 no + comp.	-1.15 to -0.19 strong, and $+0.37$ to ? weak				
21	−comp. at -0.35 no + comp.	-1.05 to -0.25 strong, and $+0.49$ to ? very weak	-1.29 to -0.29 strong, and $+0.34$ to ? weak	0.00 to $+0.41$	0.00 to $+1.49$	($K'=23$:) 0.00 to $+0.64$
25	−comp. at -0.34 no + comp.	-0.91 to -0.47 strong, with $+0.36$ to ? very broad and weak	-1.24 to -0.37 strong, with + comp. very weak	0.00 to $+0.36$	($K'=24$:) 0.00 to $+1.50$	0.00 to $+0.58$

upper electronic state. One might anticipate a rather large and unique Zeeman effect in this band, then, and so there is. In Table V we list briefly some of our measurements, and in Fig. 3*C* an enlargement of a portion of one of the spectrograms illustrates the principal pattern types obtained. The measurements are confined mostly to the R branch lines, since the overlapping of the patterns from the rather closely packed lines in the P branches makes their analysis hopeless at this dispersion.

It will be noticed that the P_1 and R_1 lines of low K values are unaffected by the field, but that the P_2 and R_2 lines become rather broad doublets. At about the level $K'=8$ the field patterns change, and take on a form which they retain out to the highest K level observed. The R_1 lines (parallel S and K) become rather diffuse doublets, the red and violet components being at first of about the same intensity, and with the outer edge of each component at about $\Delta\nu_n$ displacement from the no-field position. As K increases, however, the violet component becomes much weaker and the red component becomes narrower and somewhat stronger. The characteristic pattern for all the corresponding R_2 lines (anti-parallel S and K), on the other hand, is just one block of unresolved lines, shading from the no-field position toward higher frequency for an interval of about $\Delta\nu_n$. All patterns appear in both polarizations, although the widths and intensities are perhaps different on the two plates.

These patterns for the higher rotational levels are quite similar to those found in a $^2\Pi$ state for which there is a normal magnetic moment associated with the component of L in the direction of the electric axis. In the upper $^2\Sigma$ electronic state of this $^2\Sigma\rightarrow{}^2\Sigma$ band there is a large magnetic interaction energy between S and an internal field directed along the nuclear rotational axis. This field must be due to a component of L in this direction, the order of magnitude of this component being at least a full unit of angular momentum, for one can interpret these patterns as being the superposition of the pattern due to the symmetrical top on a partial uncoupling of the spin S. The width of the blocks of lines forming the components in the patterns decreases with increasing K, as they should. And the strength of the $-$ components for the R_1 lines and the $+$ components for the R_2 lines is just as found in the $^2\Pi\rightarrow{}^2\Sigma$ band, for these components originate in the "wing" transitions which we have discussed above.

It is not probable that this magnetic moment in this $^2\Sigma$ state could be due to nuclear rotation, for then one would expect similar very large ρ-type doubling in all $^2\Sigma$ states of this and like molecules. Now there is other reason to believe that the outer electron configuration in this $^2\Sigma$ state[11] is $4s\sigma^2 3d\sigma$, this level being derived from the low-lying $3D$ level of the Ca atom. Since $L=2$ (due to the d electron) and the effect of the electric axis is small ($\lambda=\sigma=0$), there is a good chance that the component of L along the perpendicular axis can become large. The accompanying magnetic moment and rather large coupling energy with the S then account for the Zeeman patterns observed.

[11] R. S. Mulliken, Phys. Rev. **33,** 730 (1929).

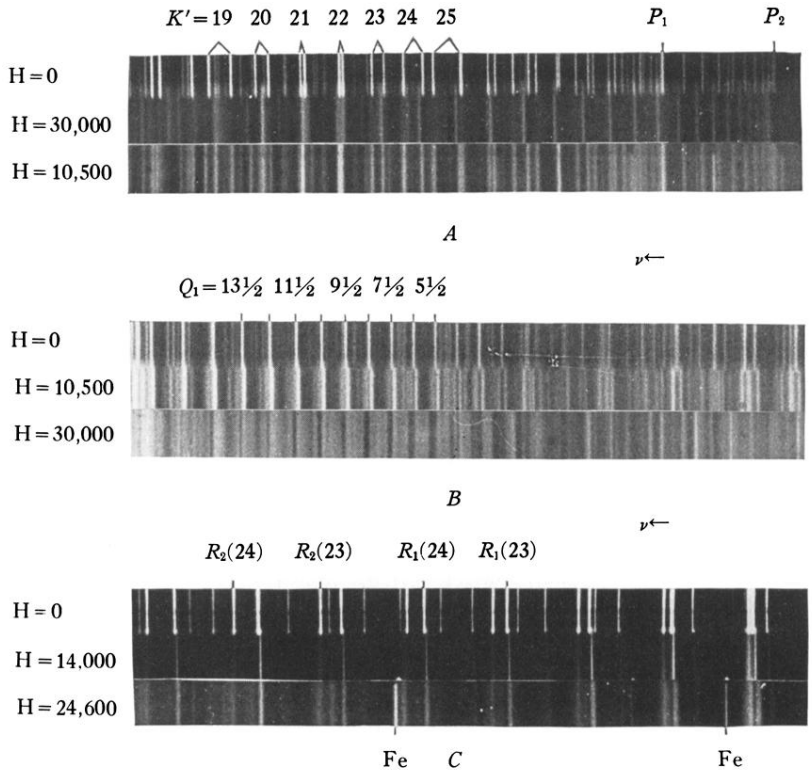

Fig. 3. Enlargements 9 times. A shows the "cross-over" region in the P branches of the $^2\Pi \rightarrow {}^2\Sigma$ band. It is evident that for $K' > 24$ both the P_1 and P_2 lines for $H = 10{,}500$ gauss have "inside" component blocks equally strong, but that for $H = 30{,}000$ gauss the P_1 field radiation has broadened out and become of negligible intensity, although the P_2 components are strong. In the reproduction P_1 and P_2 denote the heads of the two branches in the no-field strip. In B note the greater intensity of the field components on the long wave length side for $H = 10{,}500$ gauss as compared to the equal intensity of the two field components for $H = 30{,}000$ gauss. In the latter case the greater intensity of the field blocks at their inside edges is evident. C gives some of the patterns for high K values in the $^2\Sigma \rightarrow {}^2\Sigma$ band. The R_2 line patterns and the weak components of the R_1 lines on the high frequency side are of insufficient intensity to be brought out well in the reproduction. The breadth of the no-field lines in C is due to over exposure.